34 Hironaga M, Ikeda R, Fukazawa Y, Watanabe S. Mating types and serotypes of *Cryptococcus neoformans* isolated in Japan. *Sabouraudia* 1983; **21**: 73–78.
35 Kohno S, Varma A, Kwon-Chung KJ, Hara K. Epidemiology studies of clinical isolates of *Cryptococcus neoformans* of Japan by restriction fragment length polymorphism. *Kansenshogaku Zasshi* 1994; **68**: 1512–1517.
36 Okamoto K, Hatakeyama S, Itoyama S, *et al. Cryptococcus gattii* genotype VGIIa infection in man, Japan, 2007. *Emerg Infect Dis* 2010; **16**: 1155–1157.
37 Varma A, Swinne D, Staib F, Bennett JE, Kwon-Chung KJ. Diversity of DNA fingerprints in *Cryptococcus neoformans*. *J Clin Microbiol* 1995; **33**: 1807–1814.
38 Litvintseva AP, Marra RE, Nielsen K, *et al.* Evidence of sexual recombination among *Cryptococcus neoformans* serotype A isolates in sub-Saharan Africa. *Eukaryot Cell* 2003; **2**: 1162–1168.
39 Litvintseva AP, Mitchell TG. Most environmental isolates of *Cryptococcus neoformans* var. *grubii* (serotype A) are not lethal for mice. *Infect Immun* 2009; **77**: 3188–3195.

Med Mycol Downloaded from informahealthcare.com by Nagasaki University on 08/19/12
For personal use only.

RIGHTSLINK

Jpn. J. Infect. Dis., 66, 51-55, 2013

Original Article

Determination of Epidemiology of Clinically Isolated *Cryptococcus neoformans* Strains in Japan by Multilocus Sequence Typing

Takashi Umeyama[1], Hideaki Ohno[1]*, Fujihiko Minamoto[2], Taeko Takagi[3], Chiyoko Tanamachi[4], Koichi Tanabe[1], Yukihiro Kaneko[1], Satoshi Yamagoe[1], Kazuma Kishi[5], Takeshi Fujii[6], Hiromu Takemura[7], Hiroshi Watanabe[8], and Yoshitsugu Miyazaki[1]

[1]*Department of Chemotherapy and Mycoses, National Institute of Infectious Diseases, Tokyo 162-8640;*
[2]*Department of Laboratory Medicine, Microbiological Division, The Institute of Medical Science Hospital, The University of Tokyo, Tokyo 108-8639;*
[3]*Department of Laboratory Medicine and* [7]*Department of Microbiology, St. Marianna University School of Medicine, Kanagawa 216-8511;*
[4]*Department of Clinical Laboratory Medicine, Kurume University Hospital, Fukuoka 830-0011;*
[5]*Department of Respiratory Medicine, Respiratory Center, Toranomon Hospital, Tokyo 105-8470;*
[6]*Department of Infectious Diseases, Tokyo Medical University Hachioji Medical Center, Tokyo 193-0998; and*
[8]*Division of Infectious Diseases, Department of Infectious Medicine, Kurume University School of Medicine, Fukuoka 830-0011, Japan*

(Received September 14, 2012. Accepted November 30, 2012)

SUMMARY: *Cryptococcus neoformans* and *Cryptococcus gattii* are the causative agents of cryptococcosis. Despite its importance, our knowledge of the epidemiology of cryptococcosis in Japan remains limited. To establish an epidemiological database on cryptococcosis in Japan, we determined the genetic variability of 44 Japanese clinical isolates of *C. neoformans* (*var. grubii*: serotype A) by multilocus sequence typing (MLST). The strains were clinically isolated from 1992 to 2011 in 5 different areas of Japan (the Hokkaido region [n = 1], Kanto region [n = 32], Chubu region [n = 1], Kansai region [n = 1], and Kyushu region [n = 9]). According to the method recommended by the International Society for Human and Animal Mycology cryptococcal genotyping working group, 36 isolates (82%) were identified as sequence type (ST)46. The remaining strains belonged to ST45 (n = 1) and ST47 (n = 1), and 6 isolates belonged to novel independent STs. There was little geographic difference in the ST population. Our present data are still limited; however, because most clinical isolates showed the same MLST profile in Japan, applying the current MLST scheme for *Cryptococcus* may at times be insufficient for investigating the infection route among outbreak cases. To solve this problem, it may be necessary to investigate other gene loci or develop a novel method with greater discriminatory power. However, in cases in which a strain belongs to a minor ST, our data may serve as useful epidemiological information in Japan.

INTRODUCTION

Cryptococcosis is a systemic mycosis caused by the haploid, encapsulated, basidiomycetous yeast *Cryptococcus neoformans* (serotypes A, D, and AD) and *Cryptococcus gattii* (serotypes B and C), which are commonly associated with pigeon excreta and plant materials. Cryptococcosis typically involves lung diseases and central nervous system infection. *C. neoformans* causes approximately 1 million cases of meningitis globally per year in human immunodeficiency virus (HIV)-infected patients, resulting in approximately 624,700 deaths within 3 months after infection (1).

C. neoformans is presently divided into 2 varieties: *C. neoformans* var. *grubii* (serotype A) and *C. neoformans* var. *neoformans* (serotype D) (2). In addition, diploid and aneuploid AD hybrids have been isolated from the environment and patients (3,4). *C. neoformans* var. *grubii* is responsible for more than 90% cases of cryptococcosis worldwide (5). The sexual reproduction of *Cryptococcus* has a two-allele mating system comprising MATa and MATα (6). The α mating type of *C. neoformans* is predominant among clinical and environmental isolates (>98%–99.9%) (5). Mating basically occurs between opposite mating types. Recently, unisexual mating between 2 α cells has been suggested to occur naturally in *C. gattii* (7) and *C. neoformans* (8).

Genotypic analysis such as M13 DNA fingerprinting, amplified fragment length polymorphism, and multilocus sequence typing (MLST) of *C. neoformans* var. *grubii* has identified 3 molecular types: VNI, VNII, and

*Corresponding author: Mailing address: Department of Chemotherapy and Mycoses, National Institute of Infectious Diseases, 1-23-1 Toyama, Shinjuku-ku, Tokyo 162-8640, Japan. Tel: +81 3 5285 1111, Fax: +81 3 5285 1272, E-mail: h-ohno@nih.go.jp

VNB (9–13). VNI strains are globally dominant, and VNII isolates are less common. VNB is a novel molecular type discovered as a unique cryptococcal population in Botswana (13).

Recently, a standardized MLST scheme for *C. neoformans* and *C. gattii* has been established by the Cryptococcal Working Group I (Genotyping of *C. neoformans* and *C. gattii*) of the International Society for Human and Animal Mycology (ISHAM) to enable global standardization and overcome problems arising from interlaboratory reproducibility (10). The scheme uses 7 unlinked genetic loci, including the housekeeping genes *CAP59*, *GPD1*, *LAC1*, *PLB1*, *SOD1*, and *URA5* and the IGS1 region. Based on the ISHAM scheme, 183 clinical and environmental isolates from Thailand and 77 isolates from the global collection of *C. neoformans* var. *grubii* were analyzed, and the MLST database was established (14). The majority of Thailand isolates exhibit 3 sequence types (STs): ST44 (33%, n = 70), ST45 (43%, n = 78), and ST46 (14%, n = 26). ST44 and ST45 are unique to Thailand, and ST46 has been identified in Thailand and Japan (14). A recent epidemiological report has shown that 31 of the 35 *C. neoformans* var. *grubii* isolates from non-HIV patients in Nagasaki, Japan exhibited the same ST based on MLST using the same 7 loci as those used in the ISHAM scheme (15).

In Japan, cryptococcosis caused by *C. neoformans* occurs in all regions. Despite its importance, our knowledge of the epidemiology of cryptococcosis in Japan remains limited. The establishment of an epidemiological database on cryptococcosis in Japan is urgently required to manage epidemics and potential outbreaks of cryptococcosis. In this study, we used MLST, a rapid, reproducible, and discriminatory methodology for genotyping isolates of *C. neoformans* to investigate the genetic relatedness among isolates from several medical facilities in Japan. The MLST database constructed in this study could be a useful resource for global epidemiologic studies and for the recognition and tracking of the inter or intrahospital spread of *C. neoformans*.

MATERIALS AND METHODS

Clinical isolates: Forty-four clinical isolates of *C. neoformans* var. *grubii* were collected from 11 facilities from 5 regions comprising 8 prefectures in Japan. The regional distribution of the isolates was as follows: 1 clinical isolate was collected from 1 facility in the Hokkaido region, 32 clinical isolates were collected from 5 facilities in the Kanto region, 1 clinical isolate was collected from 1 facility in the Chubu region, 1 clinical isolate was collected from 1 facility in the Kansai region, and 9 clinical isolates were collected from 3 facilities in the Kyushu region (Table 1, Fig. 1). Species identification was initially performed by sequencing internal transcribed spacer (ITS) 1–2 and D1/D2 26S ribosomal DNA (rDNA) sequences.

DNA extraction: The isolates were cultured in liquid yeast extract-peptone-dextrose (YPD) medium at 30°C. DNA was extracted from the collected cells using Dr. GenTLE (TakaraBio, Otsu, Japan). Alternatively, a suspension of freshly grown cells was prepared in lysis buffer (DNeasy kit; QIAGEN, Valencia, Calif., USA) and subjected to mechanical lysis using a Multi-Beads Shocker (Yasui Kikai, Osaka, Japan). DNA was then purified from the lysed cells using the DNeasy kit (QIAGEN) according to the manufacturer's protocol.

Serotype and mating type analysis: The mating type of each isolate was determined by 4 different polymerase chain reaction (PCR) amplification reactions. Primers specific to the MATα or MATa allele of the *STE20* locus for either serotype A or D isolates were used, namely primers JOHE7270 and JOHE7272 (aA), JOHE7273/JOHE7275 (aD), JOHE7264/JOHE7265 (αA), and JOHE7267/JOHE7268 (αD), as described previously (16).

MLST analysis: MLST analysis was essentially performed according to a previously described protocol (10). Each isolate was PCR amplified in 30 μl of reaction volumes for each of the 7 MLST loci using MightyAmp (TakaraBio). The primers used in this study are the same as a previously described protocol (10), except that a primer LAC1R2 (5′-TCGGACTA TTAATCTCCAAACTC) was used instead of the primer LAC1R (10). The PCR reaction procedure included denaturation at 94°C for 2 min, followed by 40 cycles of 94°C for 10 s, 60°C for 15 s, and 68°C for 1 min for all the primers. PCR products were run on 1% agarose gel and purified using the DNA purification kit (TakaraBio). Each locus was subsequently sequenced using the Applied Biosystems 3730 sequencer with the BigDye Terminator cycle sequencing kit v3.1 (Applied Biosystems, Foster City, Calif., USA) or by ordering from FASMAC Co., Atsugi, Japan. Sequences were manually edited using EnzymeX (mekentosj.com). Alleles at each locus were assigned numbers (allele types: ATs) in comparison with those identified in the global collection (13). All nucleotide sequences obtained in this study, including novel ATs, were deposited in the DNA Data Bank of Japan (DDBJ accession nos. AB744719–AB745026). Each unique allelic profile was concatenated and assigned an ST using the archived online *C. neoformans* database on MLST.net (http://cneoformans.mlst.net/) (14).

Phylogenetic analysis: Evolutionary analyses were performed on concatenated sequences from 7 loci (*CAP59*, *GPD1*, *LAC1*, *PLB1*, *SOD1*, *URA5*, and IGS1) in MEGA5 (17). The evolutionary history was inferred by the maximum-likelihood method based on the Tamura-Nei model (18).

RESULTS

All the 44 isolates collected in this study belonged to serotype A and mating type α according to PCR classification. Sequence data were obtained for all the 44 Japanese *C. neoformans var. grubii* isolates typed at the 7 loci (Table 1). The 7 loci yielded 26 ATs (*CAP59*, 4; *GPD1*, 3; IGS1, 3; *LAC1*, 5; *PLB1*, 4; *SOD1*, 3; and *URA5*, 4), 3 of which were novel loci (*LAC1*, *SOD1*, and *URA5*). The novel AT of *LAC1* (accession no. AB744879) is the closest to AT 1 (addition of C to AT1), the novel AT of *SOD1* (accession no. AB744945) is the closest to AT12 (addition of GGA to AT12), and the novel AT of *URA5* (accession no. AB744994) is the closest to AT1 (replacement of A with C).

We identified 9 multilocus STs within the Japanese

Table 1. Clinical isolates in this study

Strain ID no.	Region	Facility	Isolated year	Serotype	Mating type	AT[1]							ST[1]
						CAP59	*GPD1*	IGS1	*LAC1*	*PLB1*	*SOD1*	*URA5*	
NIIDCr0001	Hokkaido	A	2011	A	α	1	3	19	5	2	13	1	46
NIIDCr0002	Kanto	B	1992	A	α	1	3	19	5	2	13	1	46
NIIDCr0003	Kanto	B	1993	A	α	1	3	19	5	2	13	1	46
NIIDCr0004	Kanto	B	1994	A	α	1	3	19	5	2	13	1	46
NIIDCr0005	Kanto	B	1994	A	α	1	3	19	5	2	13	1	46
NIIDCr0006	Kanto	B	1995	A	α	1	3	19	5	2	13	1	46
NIIDCr0007	Kanto	B	1997	A	α	10	9	21	8	11	Nov	4	Nov
NIIDCr0008	Kanto	B	2000	A	α	1	3	19	5	2	13	1	46
NIIDCr0009	Kanto	B	2001	A	α	1	3	19	5	2	13	1	46
NIIDCr0010	Kanto	B	2006	A	α	1	1	20	3	4	13	1	47
NIIDCr0011	Kanto	B	2008	A	α	1	3	19	5	2	13	1	46
NIIDCr0012	Kanto	C	2011	A	α	1	3	19	5	2	13	Nov	Nov
NIIDCr0013	Kanto	D	2005	A	α	1	1	19	4	2	13	5	45
NIIDCr0014	Kanto	D	2006	A	α	1	1	20	3	2	13	1	Nov
NIIDCr0015	Kanto	D	2007	A	α	1	3	19	5	2	13	1	46
NIIDCr0016	Kanto	D	2008	A	α	1	3	19	5	2	13	1	46
NIIDCr0017	Kanto	D	2008	A	α	1	3	19	5	2	13	1	46
NIIDCr0018	Kanto	D	2009	A	α	2	9	21	8	11	14	4	Nov
NIIDCr0019	Kanto	D	2009	A	α	1	3	19	5	2	13	1	46
NIIDCr0020	Kanto	D	2010	A	α	1	3	19	5	2	13	1	46
NIIDCr0021	Kanto	E	2005	A	α	1	3	19	5	2	13	1	46
NIIDCr0022	Kanto	E	2005	A	α	1	3	19	5	2	13	1	46
NIIDCr0023	Kanto	E	2008	A	α	1	3	19	5	2	13	1	46
NIIDCr0024	Kanto	E	2010	A	α	1	3	19	5	2	13	1	46
NIIDCr0025	Kanto	E	2010	A	α	1	3	19	5	2	13	1	46
NIIDCr0026	Kanto	E	2010	A	α	1	3	19	5	2	13	1	46
NIIDCr0027	Kanto	E	2011	A	α	1	3	19	5	2	13	1	46
NIIDCr0028	Kanto	E	2002	A	α	1	3	19	5	2	13	1	46
NIIDCr0029	Kanto	E	2004	A	α	7	1	19	Nov	1	13	1	Nov
NIIDCr0030	Kanto	E	2010	A	α	1	3	19	5	2	13	1	46
NIIDCr0031	Kanto	E	2011	A	α	1	3	19	5	2	13	1	46
NIIDCr0032	Kanto	E	2011	A	α	1	3	19	5	2	13	1	46
NIIDCr0033	Kanto	F	2010	A	α	1	3	19	5	2	13	1	46
NIIDCr0034	Kyushu	G	2008	A	α	1	3	19	5	2	13	1	46
NIIDCr0035	Kyushu	G	2008	A	α	1	3	19	5	2	13	1	46
NIIDCr0036	Kyushu	G	2008	A	α	7	1	19	5	1	13	1	Nov
NIIDCr0037	Kyushu	G	2008	A	α	1	3	19	5	2	13	1	46
NIIDCr0038	Kyushu	G	2008	A	α	1	3	19	5	2	13	1	46
NIIDCr0039	Kyushu	G	2009	A	α	1	3	19	5	2	13	1	46
NIIDCr0040	Kyushu	G	2009	A	α	1	3	19	5	2	13	1	46
NIIDCr0041	Kyushu	H	2011	A	α	1	3	19	5	2	13	1	46
NIIDCr0042	Chubu	I	2011	A	α	1	3	19	5	2	13	1	46
NIIDCr0043	Kansai	J	2011	A	α	1	3	19	5	2	13	1	46
YC-13	Kyushu	Nagasaki Univ.	Ref. (21)	A	α	1	3	19	5	2	13	1	46

[1]: Nov, novel AT and ST.

isolates, consisting of ST45, ST46, ST47, and 6 novel STs. Thirty-six of the 44 isolates belonged to ST46 (81%) (Table 1). The remaining strains belonged to ST45 (n = 1) and ST47 (n = 1), and 6 isolates belonged to novel independent STs. A phylogenetic tree was constructed by the maximum-likelihood method based on a concatenated data set from 7 loci for MLST (Fig. 2). Among the novel STs, 2 strains (NIIDCr0007 and NIIDCr0018) were located in a different cradle, which indicated the VNII genetic type. The other 42 strains belonged to the VNI type, a major type of *C. neoformans*. No clinical isolate belonged to the VNB type.

From a geographic perspective, 27 of 34 isolates (79%) from Eastern Japan, including the Hokkaido, Kanto, and Chubu regions, and 9 of 10 isolates (90%) from Western Japan, including the Kansai and Kyushu regions, belonged to ST46, indicating that there is little geographical bias between Eastern and Western Japan in the contributions of ST46 isolates (Fisher's exact test; P = 0.659). Two isolates (NIIDCr0007 and NIIDCr0018), which belong to the molecular type VNII, were isolated from the Kanto region of Eastern Japan.

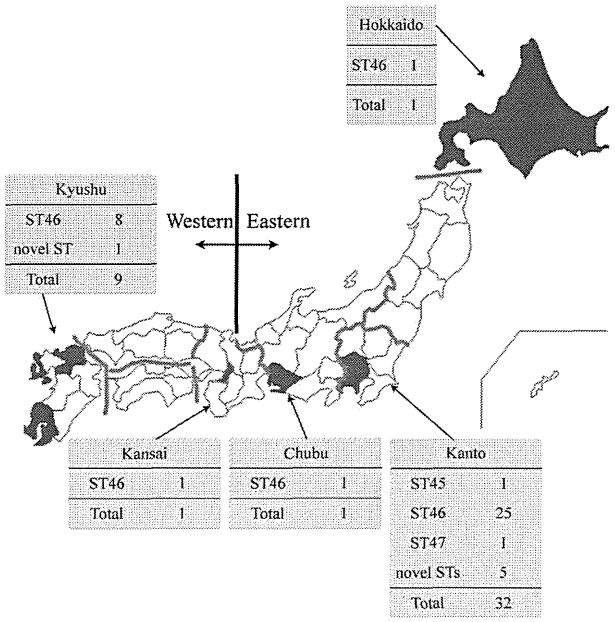

Fig. 1. Map of Japan showing the distribution of multilocus sequence typing (MLST) profile and the number of isolates according to the region involved in the study. Details are shown in Table 1.

DISCUSSION

There are no previous studies of MLST epidemiology by the ISHAM standard method for clinical isolates of *C. neoformans* var. *grubii* obtained from multiple facilities in Japan. In this study, we analyzed 44 clinical strains of *C. neoformans* from 11 facilities. Most isolates were classified as the same ST, ST46 (81%). This result indicates that it may be difficult to predict the origin of potential cryptococcosis outbreaks using the MLST scheme if the isolates belong to ST46. However, STs of other isolates are phylogenetically independent of each other (Fig. 2), and these minor STs will be useful for global epidemiologic studies, recognition, and tracking the inter or intrahospital spread of *C. neoformans* in Japan.

A recent epidemiological study has shown that clinical and environmental isolates in Thailand predominantly consist of 3 STs, ST44, ST45, and ST46, accounting for up to 90% of the total isolates investigated (14), indicating low genetic diversity. In Japan, Mihara et al. (15) has reported that 31 of the 35 isolates in Nagasaki, Japan exhibited ST5. ST46 in this study and ST5 in the study of Mihara et al. are derived from the same nucleotide sequences in the 7 loci. This discrepancy of ST might be due to the MLST database;

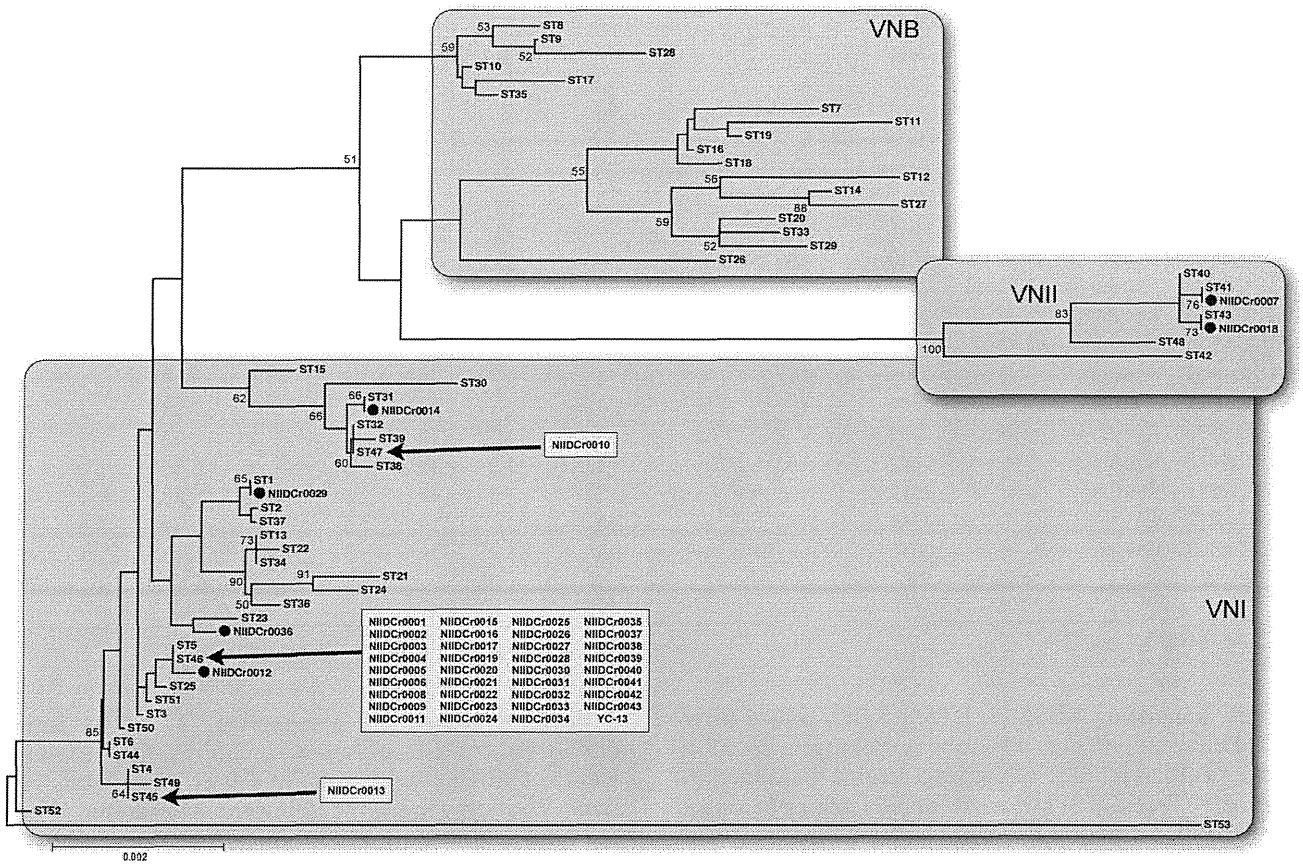

Fig. 2. Molecular phylogenetic analysis by the maximum-likelihood method of the 44 Japanese clinical isolates and known sequence types (STs) of *Cryptococcus neoformans* using a concatenated data set derived from seven loci (*CAP59*, *GPD1*, *LAC1*, *PLB1*, *SOD1*, *URA5*, and IGS1). The tree with the highest log likelihood (−7730.9017) is shown and drawn to scale, with branch lengths measured in the number of substitutions per site. The percentage (>50%) of trees in which the associated taxa clustered together is shown next to the branches. Analysis involved 61 nucleotide sequences. There were 3901 positions in the final dataset. VN molecular types (VNI, VNII, and VNB) are represented by gray rectangles.

http://cneoformans.mlst.net and http://mlst.mycology lab.org are used for this study and the study of Mihara et al., respectively. To compare STs in this study with the large-scale investigation by Simwami et al. (14), we adopted the former database. A Chinese epidemiological study has shown that the majority of *C. neoformans* isolates exhibited the same ST, in which the nucleotide sequences of 5 loci examined (*GPD1*, IGS1, *LAC1*, *PLB1*, and *SOD1*) are identical to those of ST46 (19). Similarly, the nucleotide sequences of all 7 loci in the major ST of clinical isolates in Korea are the same as those of ST46 in this study (20). Together, ST46, a predominant ST in Japan (determined in this study), has so far been isolated in Thailand, China, Korea, and Japan, which are geographically close to each other, suggesting that ST46 isolates from Asia may have the same origin.

Seven strains from the facility G in the Kyushu region (NIIDCr0034–0040) were isolated within a year (2008–2009). Usually, this facility only diagnoses 1 or 2 cases of cryptococcosis per year. Therefore, the high frequency of cryptococcosis could indicate a possibility of outbreaks occurring in the vicinity of the facility G. MLST analysis of these 7 isolates in this study revealed that 6 isolates belong to ST46. The cases at the facility E in the Kanto region showed similar patterns: 7 strains (NIIDCr0024–0027 and 0030–0032) were isolated in 1 year (2010–2011) and 6 isolates exhibited ST46. Local molecular epidemiology restricted to a small area should be able to indicate that these 2 cases were potential outbreaks; however, using our cryptococcal MLST database, the ST46 strain can be recognized as the predominant strain type that is widespread in Japan. Therefore, the present MLST analysis seems less useful for predicting or tracing the infection route or infection source of cryptococcosis outbreaks in Japan. To investigate the actual origin of these outbreaks, novel epidemiological tools such as multilocus microsatellite typing and whole genome sequencing will be required.

In conclusion, we analyzed clinical isolates of *C. neoformans* obtained from multiple locations widely distributed in Japan by MLST, a molecular epidemiological method. Most clinical isolates belong to the same ST (ST46), and there is little geographic bias among the areas studied. This database will be useful for public health officials in designing and prioritizing efforts to prevent, diagnose, and treat cryptococcal disease.

Acknowledgments The authors would like to thank Hiroko Kusachi for the technical support. We also thank medical doctors; Akiko Takeuchi, Masaki Ohyagi, Etsuko Sawabe, Noboru Takayanagi, Naho Kagiyama, Kazumitsu Sugiura, Masatomo Kimura, Shigeru Kohno, and Hideki Kawamura, who provided us with *C. neoformans* isolates.

This work was supported by grants from the Ministry of Health, Labour and Welfare of Japan (H24-shinkou-ippan-013, H23-shinkou-ippan-007, H23-shinkou-ippan-018, H22-shinko-ippan-008, and H21-shinkou-ippan-009).

Conflict of interest None to declare.

REFERENCES

1. Park, B.J., Wannemuehler, K.A., Marston, B.J., et al. (2009): Estimation of the current global burden of cryptococcal meningitis among persons living with HIV/AIDS. AIDS, 23, 525–530.
2. Franzot, S.P., Salkin, I.F. and Casadevall, A. (1999): *Cryptococcus neoformans* var. *grubii*: separate varietal status for *Cryptococcus neoformans* serotype A isolates. J. Clin. Microbiol., 37, 838–840.
3. Lengeler, K.B., Cox, G.M. and Heitman, J. (2001): Serotype AD strains of *Cryptococcus neoformans* are diploid or aneuploid and are heterozygous at the mating-type locus. Infect. Immun., 69, 115–122.
4. Xu, J., Luo, G., Vilgalys, R.J., et al. (2002): Multiple origins of hybrid strains of *Cryptococcus neoformans* with serotype AD. Microbiology, 148, 203–212.
5. Heitman, J., Kozel, T.R., Kwon-Chung, K.J., et al. (2010): *Cryptococcus* from Human Pathogen to Model Yeast. ASM Press, Washington, D.C.
6. Kwon-Chung, K.J. and Bennett, J.E. (1978): Distribution of α and a mating types of *Cryptococcus neoformans* among natural and clinical isolates. Am. J. Epidemiol., 108, 337–340.
7. Fraser, J.A., Giles, S.S., Wenink, E.C., et al. (2005): Same-sex mating and the origin of the Vancouver Island *Cryptococcus gattii* outbreak. Nature, 437, 1360–1364.
8. Lin, X., Litvintseva, A.P., Nielsen, K., et al. (2007): αADα hybrids of *Cryptococcus neoformans*: evidence of same-sex mating in nature and hybrid fitness. PLoS Genet., 3, 1975–1990.
9. Meyer, W., Castañeda, A., Jackson, S., et al. (2003): Molecular typing of IberoAmerican *Cryptococcus neoformans* isolates. Emerg. Infect. Dis., 9, 189–195.
10. Meyer, W., Aanensen, D.M., Boekhout, T., et al. (2009): Consensus multi-locus sequence typing scheme for *Cryptococcus neoformans* and *Cryptococcus gattii*. Med. Mycol., 47, 561–570.
11. Bovers, M., Hagen, F., Kuramae, E.E., et al. (2008): Six monophyletic lineages identified within *Cryptococcus neoformans* and *Cryptococcus gattii* by multi-locus sequence typing. Fungal Genet. Biol., 45, 400–421.
12. Ngamskulrungroj, P., Gilgado, F., Faganello, J., et al. (2009): Genetic diversity of the *Cryptococcus* species complex suggests that *Cryptococcus gattii* deserves to have varieties. PLoS ONE, 4, e5862.
13. Litvintseva, A.P., Thakur, R., Vilgalys, R., et al. (2006): Multilocus sequence typing reveals three genetic subpopulations of *Cryptococcus neoformans* var. *grubii* (serotype A), including a unique population in Botswana. Genetics, 172, 2223–2238.
14. Simwami, S.P., Khayhan, K., Henk, D.A., et al. (2011): Low diversity *Cryptococcus neoformans* variety *grubii* multilocus sequence types from Thailand are consistent with an ancestral African origin. PLoS Pathog., 7, e1001343.
15. Mihara, T., Izumikawa, K., Kakeya, H., et al. (2012): Multilocus sequence typing of *Cryptococcus neoformans* in non-HIV associated cryptococcosis in Nagasaki, Japan. Med. Mycol. Doi: 10.3109/13693786.2012.708883.
16. Barreto de Oliveira, M.T., Boekhout, T., Theelen, B., et al. (2004): *Cryptococcus neoformans* shows a remarkable genotypic diversity in Brazil. J. Clin. Microbiol., 42, 1356–1359.
17. Tamura, K. and Nei, M. (1993): Estimation of the number of nucleotide substitutions in the control region of mitochondrial DNA in humans and chimpanzees. Mol. Biol. Evol., 10, 512–526.
18. Tamura, K., Peterson, D., Peterson, N., et al. (2011): MEGA5: molecular evolutionary genetics analysis using maximum likelihood, evolutionary distance, and maximum parsimony methods. Mol. Biol. Evol., 28, 2731–2739.
19. Chen, J., Varma, A., Diaz, M.R., et al. (2008): *Cryptococcus neoformans* strains and infection in apparently immunocompetent patients, China. Emerg. Infect. Dis., 14, 755–762.
20. Choi, Y.H., Ngamskulrungroj, P., Varma, A., et al. (2010): Prevalence of the VNIc genotype of *Cryptococcus neoformans* in non-HIV-associated cryptococcosis in the Republic of Korea. FEMS Yeast Res., 10, 769–778.
21. Yasuoka, A., Kohno, S., Yamada, H., et al. (1994): Influence of molecular sizes of *Cryptococcus neoformans* capsular polysaccharide on phagocytosis. Microbiol. Immunol., 38, 851–856.

AAC
Journals.ASM.org

Real-Time Microscopic Observation of *Candida* Biofilm Development and Effects Due to Micafungin and Fluconazole

Yukihiro Kaneko,[a] Susumu Miyagawa,[b] On Takeda,[b] Masateru Hakariya,[c] Satoru Matsumoto,[d] Hideaki Ohno,[a] Yoshitsugu Miyazaki[a]

Department of Chemotherapy and Mycoses, National Institute of Infectious Diseases, Tokyo, Japan[a]; ICAM Co., Ltd., Tokyo, Japan[b]; Cine-Science Laboratory, Tokyo, Japan[c]; Pharmacology Research Laboratories, Astellas Pharma Inc., Ibaraki, Japan[d]

To understand the process of *Candida* biofilm development and the effects of antifungal agents on biofilms, we analyzed real-time data comprising time-lapse images taken at times separated by brief intervals. The growth rate was calculated by measuring the change of biofilm thickness every hour. For the antifungal study, 5-h-old biofilms of *Candida albicans* were treated with either micafungin (MCFG) or fluconazole (FLCZ). MCFG began to suppress biofilm growth a few minutes after the initiation of the treatment, and this effect was maintained over the course of the observation period. In contrast, the suppressive effects of FLCZ on biofilm growth took longer to manifest: biofilms grew in the first 5 h after treatment, and then their growth was suppressed over the next 10 h, finally producing results similar to those observed with MCFG. MCFG was also involved in the disruption of cells in the biofilms, releasing string-like structures (undefined extracellular component) from the burst hyphae. Thus, MCFG inhibited the detachment of yeast cell clusters from the tips of hyphae. In contrast, FLCZ did not disrupt biofilm cells. MCFG also showed fast antifungal activity against *Candida parapsilosis* biofilms. In conclusion, our results show that inhibition of glucan synthesis due to MCFG contributed not only to fungicidal activity but also to the immediate suppression of biofilm growth, while FLCZ suppressed growth by inhibiting ergosterol synthesis. Therefore, those characteristic differences should be considered when treating clinical biofilm infections.

Pathogenic fungi in the genus *Candida* can cause both superficial and serious systemic diseases and are now widely recognized as important agents of hospital-acquired infection (1). *Candida albicans* is known as a biofilm former. Bloodstream infections are frequently associated with the use of a catheter, and the catheter can be a scaffold for biofilms (2). Once biofilms are formed, the biofilms continuously supply detaching cells as a source of infection; thus, biofilm-related infection is associated with a poor prognosis (2, 3). Recently, research into molecular mechanisms related to biofilm formation has revealed transcriptional regulation (4); however, the majority of these related studies lack real-time observation of the development process, and therefore, the fate of the biofilm and the effects of antifungals against biofilms are not clearly understood. Knowing the mechanism of antifungal action against biofilms would provide us with key information when considering therapeutic strategy against clinical infections related to biofilms. In this study, we analyzed images obtained by time-lapse photography to investigate the developmental process and detachment of biofilms, as well as the antibiofilm effects of the echinocandin micafungin (MCFG), which inhibits cell wall glucan synthesis, and the azole fluconazole (FLCZ), which inhibits cell membrane ergosterol synthesis.

MATERIALS AND METHODS

Chemicals. All general chemicals used in this study were purchased from Wako Chemicals (Tokyo, Japan), unless otherwise indicated, and were of the highest purity available. Ultrapure water dispensed by a Milli-Q water system (Millipore, Bedford, MA) was used for the preparation of buffers and solvents. MCFG (Astellas Pharma Inc., Tokyo, Japan) and FLCZ were dissolved in double-distilled water (ddW) at 1 mg/ml for stock solutions, and both were stored at −20°C prior to use.

Strains and growth conditions. Clinical isolates of *Candida albicans* 21004 (Ca21004) and *Candida parapsilosis* 20007 (Cp20007) used in this study were stored in 20% glycerol at −80°C prior to use. Silicone disks were obtained from Dainichikougyo (Saitama, Japan) and self-manufactured to produce small pieces (approximately 1-mm by 1-mm squares, 0.3 mm thick).

Cells were grown in RPMI 1640−0.165 M morpholinepropanesulfonic acid (MOPS) (Sigma-Aldrich), and the overnight cultures were adjusted as an inoculation suspension. The small pieces of silicon disks were placed in an originally developed chamber and pretreated with fetal bovine serum at 37°C for 24 h, immersed in a cell suspension of 2×10^7 CFU/ml, and incubated at 37°C for 1 h. Following a brief wash, cells were grown in RPMI 1640−0.165 M MOPS with 20 ml/h flow using AC-2120 precision Perista pumps (ATTO, Tokyo, Japan), which were placed on both the influx and efflux sides. Biofilms were observed both from the top and the side, and those views were recorded by time-lapse images for 24 h at a rate of 1 frame per min, unless otherwise indicated. Time-lapse images were captured using a DXC-950 charge-coupled-device (CCD) color video camera (Sony, Tokyo, Japan) equipped with a Diaphot microscope (Nikon, Tokyo, Japan).

Scanning electron microscopy. Samples for electron microscopy were prepared by a method previously described (5). Briefly, 24-h-old biofilms were fixed with 2.5% glutaraldehyde–2% paraformaldehyde–0.1 M phosphate-buffered saline (PBS) for 30 min and washed with 0.1 M PBS 3 times. After dehydration through an ascending alcohol series, the specimens were processed using a freeze dryer (model ES-2030; Hitachi, Tokyo, Japan) and *tert*-butyl ethanol, coated with osmium, and examined with a scanning electron microscope (SU6600; Hitachi, Tokyo, Japan).

Received 15 November 2012 Returned for modification 19 January 2013
Accepted 25 February 2013
Published ahead of print 4 March 2013
Address correspondence to Yukihiro Kaneko, ykaneko@nih.go.jp.
Supplemental material for this article may be found at http://dx.doi.org/10.1128/AAC.02290-12.
Copyright © 2013, American Society for Microbiology. All Rights Reserved.
doi:10.1128/AAC.02290-12

Downloaded from http://aac.asm.org/ on February 3, 2014 by Natinoal Institute of Infectius Diseases, Murayama Bunshitsu

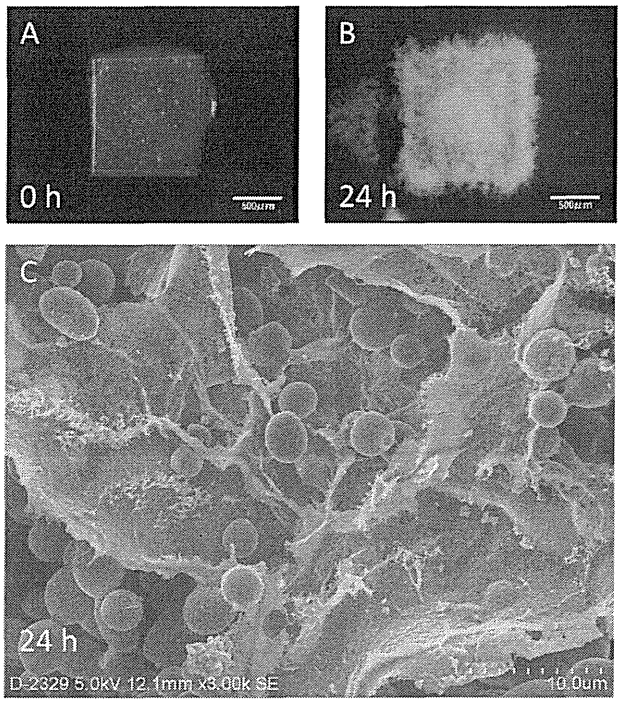

FIG 1 Development of *Candida albicans* biofilms on a silicon disk in flow, observed from the top, and the electron microscopic image. (A and B) Attachment phase (A) and 24-h-old mature biofilms (B). (C) Mature biofilms were also observed under a scanning electron microscope, revealing a dense extracellular matrix covering the accumulated *Candida* cells.

Calculation of growth rate. Time-lapse images of the side view of the biofilms were recorded for 24 h at a rate of 1 frame per min. Each frame was approximately 600 μm wide and was divided into 6 areas 100 μm in width. The peak height of each area was measured, and the values of the 6 areas were averaged to define the biofilm thickness. The biofilm thickness was calculated every hour. The growth rate was further calculated by measuring hourly changes in the biofilm thickness.

Treatment of antifungal agents. Treatment with MCFG or FLCZ was performed on 5-h-old biofilms. Ca21004 and Cp20007 were treated with 1 μg/ml and 16 μg/ml of MCFG, respectively, and Ca21004 was treated with 25 μg/ml of FLCZ. MIC values were determined by the Clinical and Laboratory Standards Institute (CLSI) reference method for broth dilution antifungal susceptibility testing of yeasts (approved standard, second edition; CLSI document M27-A3) (6). The MIC values for MCFG were ≤0.002 and 0.5 μg/ml for Ca21004 and Cp20007, respectively, and the MIC value for FLCZ was 0.25 μg/ml for Ca21004.

Treatment doses were determined based on (i) the trough value (approximately 1 μg/ml) when MCFG was administered at 50 mg/day and (ii) the value for the maximum concentration of drug in serum (C_{max}) (approximately 25 μg/ml) when fosfluconazole was administered at 1 g (800 mg FLCZ equivalent) of the loading dose (2 days) (7, 8).

Statistics. Data were analyzed by unpaired *t* tests. Statistical significances are shown as *P* values. Data are presented as the means ± standard errors (SE). Error bars represent the SE.

RESULTS

Biofilms grew at constant rate, and cell detachment occurred in clusters. Biofilms of *C. albicans* Ca21004 were allowed to develop on silicon disks in flow, beginning with the attachment phase at 0 h until significant mass was achieved at 24 h (Fig. 1A and B).

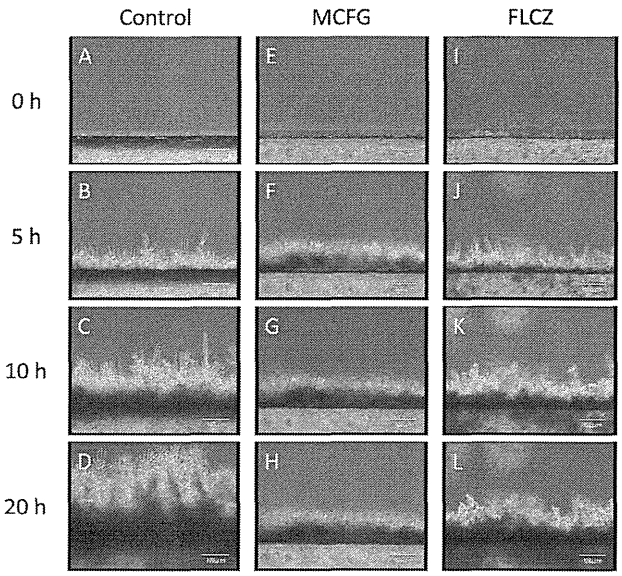

FIG 2 Development of *Candida albicans* biofilms observed from a side view, and the effects of FLCZ and MCFG. (A to D) Biofilms developed continuously; the silicon sides of biofilms were dense (dark), while the flow sides consisted mainly of hyphae. (E to L) Treatment with MCFG or FLCZ was initiated on 5-h-old biofilms. MCFG completely suppressed biofilm growth (E to H), while FLCZ partially suppressed biofilm growth (I to L).

Electron microscopy revealed that the 24-h-old biofilms included dense extracellular matrices covering aggregated cells, indicative of matured biofilms (Fig. 1C).

Observation of the continuously developing biofilms revealed that the silicon side of the biofilms became dense (dark), while the flow side consisted mainly of hyphae (Fig. 2A to D; see also movie S1A in the supplemental material). In addition, we observed detachment of small pieces of clustered cells, which had been loosely attached to the tips of hyphae in the matured biofilm (Fig. 3 and data not shown).

Biofilm thickness was measured hourly to calculate growth rate. The growth curve and growth rate are shown in Fig. 4. The average growth rate from 0 to 20 h without treatment was 17.2 ± 1.3 μm/h.

MCFG immediately suppresses biofilm growth, while FLCZ takes longer to produce an antibiofilm effect. Treatment with MCFG or FLCZ was performed on 5-h-old biofilms of *C. albicans* Ca21004. Although neither MCFG nor FLCZ eradicated biofilms from the surface of the disks, MCFG began to suppress the growth of biofilms only minutes after the start of the treatment, and the average growth rate for 5 h after addition was −0.4 ± 2.3 μm/h. The growth rate for the next 10 h was still only 0.5 ± 0.4 μm/h (Fig. 2E to H, Fig. 4). Thus, MCFG acts immediately and completely suppresses biofilm growth.

MCFG was also observed to disrupt cells in the biofilms and burst the tips of their hyphae, releasing string-like structures (undefined extracellular component) from the cells (Fig. 5).

In addition, these same effects were observed in biofilms of *C. parapsilosis* Cp21007 (Fig. 6 to 8; see also movie S2A to C in the supplemental material), though the biofilm structures were slightly different. *C. parapsilosis* biofilms did not consist of typical hyphae, but MCFG acted immediately and burst cells in biofilms, resulting in release of the contents.

Downloaded from http://aac.asm.org/ on February 3, 2014 by National Institute of Infectious Diseases, Murayama Bunshitsu

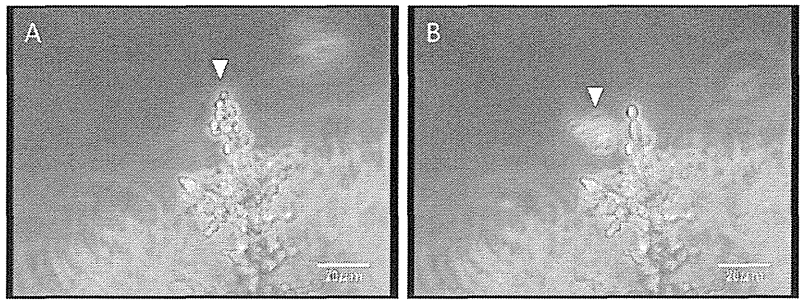

FIG 3 The moment of detachment from *Candida albicans* biofilms. In a close view from the side, a cell cluster (arrowhead) detaches from the tip of the biofilm.

In contrast, FLCZ slowly suppressed biofilm growth, with an average growth rate of 11.3 ± 3.6 μm/h for the first 5 h, followed by a growth rate of 1.1 ± 1.0 μm/h for the next 10 h (Fig. 2I to L and Fig. 4). Thus, FLCZ can also suppress biofilm growth but does so at a lower rate than MCFG and without disruption of the biofilm cells. Furthermore, FLCZ did not inhibit detachment of yeast cell clusters from the tips of the hyphae.

DISCUSSION

The growth rate of biofilms has been conventionally calculated by flow eluate, a method that may produce inaccurate results but has never been evaluated by real-time observation (9). If cell division occurs at a constant rate, cell counts increase exponentially. However, our direct observation revealed the growth of biofilms to be linear, implying that cell division is heterogenous in biofilms. These results might support the notion of the existence of persisters, which may terminate division or inhibit growth (10).

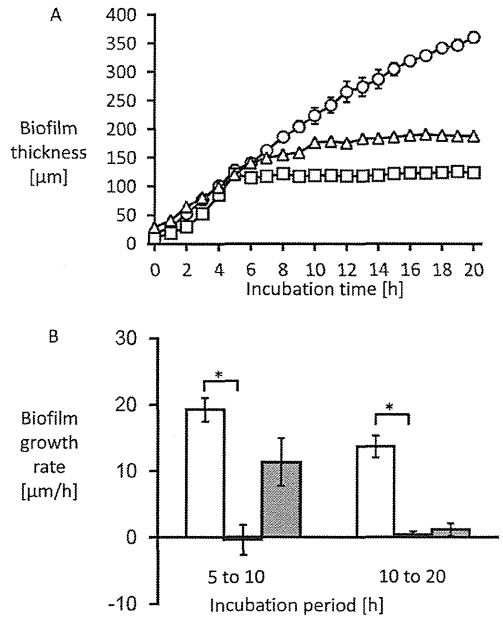

FIG 4 The thickness of *Candida albicans* biofilms was measured (A), and the growth rate was calculated by measuring the change of biofilm thickness every hour (B). (A) The untreated biofilms exhibited linear growth (circles). (B) The average growth rate at 0 to 20 h without treatment was 17.2 ± 1.3 μm/h (white bars). MCFG began to suppress biofilm growth only minutes after the start of the treatment (A [squares]). The average growth rate for the first 5 h after addition was −0.4 ± 2.3 μm/h, followed by a growth rate of 0.5 ± 0.4 μm/h for the next 10 h (B [black bars]). In contrast, FLCZ suppressed biofilm growth at a lower rate (A [triangles]), with an average growth rate for the first 5 h of 11.3 ± 3.6 μm/h, followed by a growth rate of 1.1 ± 1.0 μm/h for the next 10 h (B [gray bars]). *, $P < 0.01$.

In this study, detachment of yeast cell clusters from the tips of the hyphae was observed. In conventional models, such as *Pseudomonas aeruginosa* biofilms, planktonic cells have been shown to disperse from the centers of the biofilms (11). Moreover, a study by Blankenship et al. showed that quorum-sensing factors promote dispersal (12) and Uppuluri et al. reported that NRG1, a transcriptional regulator, controls the dispersion (13). However, our flow model shows that cell detachment occurs near the surface as a cluster. Therefore, cell detachment seems to occur passively in a cluster as a result of shear stress rather than by signal-induced dispersal.

The present study also clarified the antifungal effect of MCFG and FLCZ. MCFG is well known as a fungicidal for plankton because it can eradicate biofilm, while FLCZ is fungistatic for plankton and cannot eradicate biofilms even at extremely high concentrations (14, 15). In this study, MCFG suppressed biofilm growth within minutes of the start of the treatment, and these effects persisted throughout the observation period. This rapid effect by MCFGs presents clinical advantages for its use. In addition, MCFG was responsible for disruption of cells in the biofilms and for bursting the tips of their hyphae. Further evaluation is required to understand the entire effect of MCFG on biofilms, but these current results are consistent with those of previous studies demonstrating the biofilm-eradicating effects of MCFG (14, 16). Furthermore, the bursting activity we observed may further contribute to biofilm eradication. Similar effectiveness was observed in biofilms of *C. parapsilosis*, which is known frequently to cause biofilm-related infections such as line infections (17). Therefore, MCFG may be expected to shown efficacy against candidiasis, including such biofilm infections.

In a recent related study, Valentín et al. reported that voriconazole displayed the ability to reduce the formation of biofilms when it was present during biofilm formation or when biofilms were allowed to form on surfaces previously coated with the drug (18). Our results suggest that azoles are capable of suppressing biofilm growth at clinically achievable concentrations, although it should be noted that a lack of azole activity against preformed *Candida* biofilms has been reported (14, 15, 19). Methodological differences may contribute to the divergence between our data and other published data. Previous methodologies, for example, bio-

Downloaded from http://aac.asm.org/ on February 3, 2014 by Natinoal Institute of Infectius Diseases, Murayama Bunshitsu

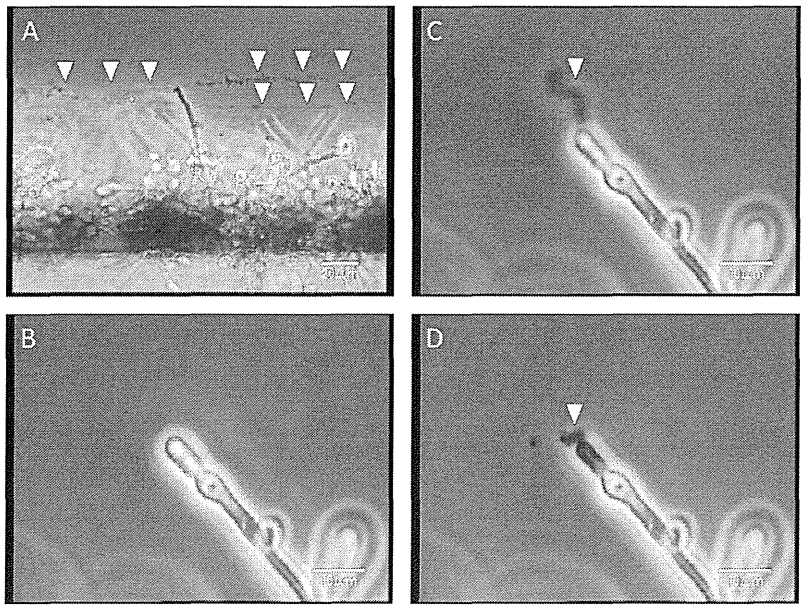

FIG 5 MCFG disrupted cells in the *Candida albicans* biofilms and burst the tips of their hyphae. (A) After MCFG disrupted the cells in the biofilms, string-like structures were released from the cells (arrowheads). (B to D) A closer view reveals the ejection of material from the bursting cells (arrowheads).

film assays using XTT, are very easy to perform and thus useful when multiple samples need to be evaluated simultaneously but lack information about the growth rate and would not be able to evaluate FLCZ inhibition of *Candida* biofilm growth accurately. Our method is useful for finding the detailed mechanism of action, but it requires special apparatus and technique. Thus, it is not thought that our method will ever replace XTT or CFU counts, but real-time observation could provide us with novel findings about biofilm behavior. Thus, our data may show that the ineffectiveness of FLCZ against preformed *Candida* biofilms was due in part to the delayed activity. In addition, the delayed action of FLCZ

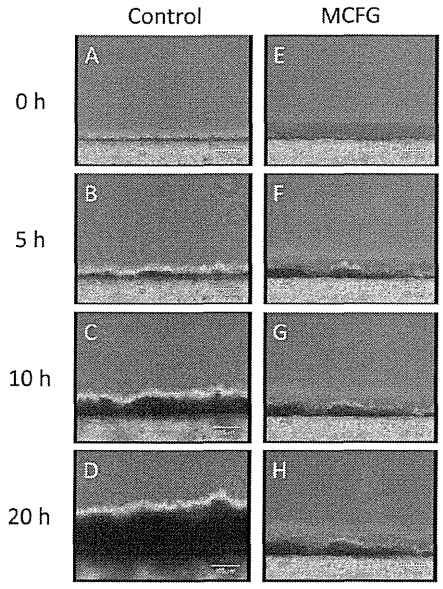

FIG 6 Development of *Candida parapsilosis* biofilms observed from a side view with and without the effect of MCFG. (A to D) Biofilms developed continuously; the silicon sides of biofilms were dense (dark); but unlike *Candida albicans*, *Candida parapsilosis* did not form hyphae. (E to H) Treatment with MCFG was initiated on 5-h-old biofilms, and MCFG completely suppressed biofilm growth.

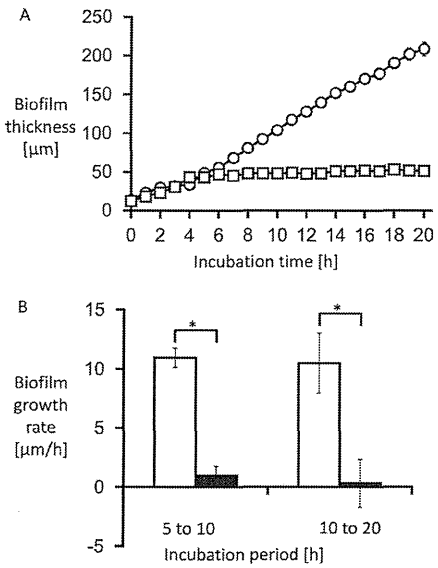

FIG 7 The thickness of *Candida parapsilosis* biofilms was measured (A), and the growth rate was calculated by measuring the change of biofilm thickness every hour (B). (A) Untreated biofilms exhibited linear growth (circles). (B) The average growth rate at 5 to 10 h without treatment was 11.0 ± 1.0 μm/h (white bars). MCFG began to suppress biofilm growth only minutes after initiation of the treatment (A [squares]). The average growth rate for 5 h after addition was 1.0 ± 1.1 μm/h, with a growth rate of 0.3 ± 0.4 μm/h for the next 10 h (B [black bars]). *, $P < 0.01$.

Downloaded from http://aac.asm.org/ on February 3, 2014 by Natinoal Institute of Infectius Diseases, Murayama Bunshitsu

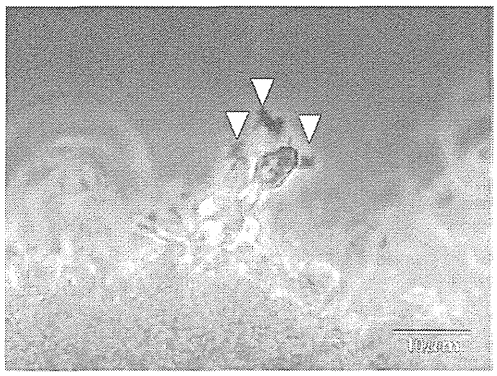

FIG 8 MCFG disrupted cells in the *Candida parapsilosis* biofilms and burst the tips of their daughter cells. MCFG disrupted cells in the biofilms, and string-like contents of cells (arrowheads) were released from a bursting cell.

against *Candida* biofilms might be due to preexistent ergosterol that was to some extent pooled in the cell.

When we evaluated the biofilm growth, other parameters, including biomass measuring, were also considered; however, biomass measurement requires special software and apparatus. Besides, this measurement of peak height was thought to reflect the intuitive observation of biofilm growth, and therefore we adopted this strategy.

In conclusion, our results show that inhibition of glucan synthesis due to MCFG contributes not only to fungicidal activity but also to the immediate suppression of biofilm growth, whereas FLCZ contributes only to suppression of biofilm growth through the inhibition of ergosterol synthesis. Therefore, those characteristic differences should be considered when treating clinical biofilm infections.

ACKNOWLEDGMENTS

This work was partly supported by grants from the Ministry of Education, Culture, Sports, Science and Technology of Japan (KAKENHI 24791032), the Japan Society for the Promotion of Grants-in-Aid for Young Scientists (B) (24791032), the Ministry of Health, Labor and Welfare of Japan (H22shinkouippan008, H23shinkouippan007, and H23shinkouippan018), and the Takeda Science Foundation.

We thank Noriko Saito for performing scanning electron microscopy.

Y.K. contributed to the overall study design and manuscript preparation. S Miyagawa, OT, and MH performed time-lapse image analysis. H.O. generally advised for the entire manuscript. S. Matsumoto and Y.M. provided overall supervision. We all approved the manuscript prior to submission.

REFERENCES

1. **Kuhn DM, Ghannoum MA.** 2004. *Candida* biofilms: antifungal resistance and emerging therapeutic options. Curr. Opin. Investig. Drugs 5:186–197.
2. **Zirkel J, Klinker H, Kuhn A, Abele-Horn M, Tappe D, Turnwald D, Einsele H, Heinz WJ.** 2012. Epidemiology of *Candida* blood stream infections in patients with hematological malignancies or solid tumors. Med. Mycol. 50:50–55.
3. **Zilberberg MD, Kollef MH, Arnold H, Labelle A, Micek ST, Kothari S, Shorr AF.** 2010. Inappropriate empiric antifungal therapy for candidemia in the ICU and hospital resource utilization: a retrospective cohort study. BMC Infect. Dis. 10:150. doi:10.1186/1471-2334-10-150.
4. **Nobile CJ, Fox EP, Nett JE, Sorrells TR, Mitrovich QM, Hernday AD, Tuch BB, Andes DR, Johnson AD.** 2012. A recently evolved transcriptional network controls biofilm development in *Candida albicans*. Cell 148:126–138.
5. **Seki N, Kasai S, Saito N, Komagata O, Mihara M, Sasaki T, Tomita T, Sasaki T, Kobayashi M.** 2007. Quantitative analysis of proliferation and excretion of *Bartonella quintana* in body lice, *Pediculus humanus* L. Am. J. Trop. Med. Hyg. 77:562–566.
6. **Clinical and Laboratory Standards Institute.** 2007. Reference method for broth dilution antifungal susceptibility testing of yeasts: approved standard, 3rd ed. CLSI document M27-A3. CLSI, Wayne, PA.
7. **Azuma J, Nakahara K, Kagayama A, Okuma T, Kawamura A, Mukai T.** 2002. Pharmacokinetic study of micafungin. Jpn. J. Chemother. 50(S-1): 155–184.
8. **Sobue S, Tan K, Layton G, Eve M, Sanderson JB.** 2004. Pharmacokinetics of fosfluconazole and fluconazole following multiple intravenous administration of fosfluconazole in healthy male volunteers. Br. J. Clin. Pharmacol. 58:20–25.
9. **Baillie GS, Douglas LJ.** 1998. Effect of growth rate on resistance of *Candida albicans* biofilms to antifungal agents. Antimicrob. Agents Chemother. 42:1900–1905.
10. **Lafleur MD, Qi Q, Lewis K.** 2010. Patients with long-term oral carriage harbor high-persister mutants of *Candida albicans*. Antimicrob. Agents Chemother. 54:39–44.
11. **Purevdorj-Gage B, Costerton WJ, Stoodley P.** 2005. Phenotypic differentiation and seeding dispersal in non-mucoid and mucoid *Pseudomonas aeruginosa* biofilms. Microbiology 151:1569–1576.
12. **Blankenship JR, Mitchell AP.** 2006. How to build a biofilm: a fungal perspective. Curr. Opin. Microbiol. 9:588–594.
13. **Uppuluri P, Pierce CG, Thomas DP, Bubeck SS, Saville SP, Lopez-Ribot JL.** 2010. The transcriptional regulator Nrg1p controls *Candida albicans* biofilm formation and dispersion. Eukaryot. Cell 9:1531–1537.
14. **Kaneko Y, Ohno H, Fukazawa H, Murakami Y, Imamura Y, Kohno S, Miyazaki Y.** 2010. Anti-*Candida*-biofilm activity of micafungin is attenuated by voriconazole but restored by pharmacological inhibition of Hsp90-related stress responses. Med. Mycol. 48:606–612.
15. **Ramage G, Vande Walle K, Wickes BL, Lopez-Ribot JL.** 2001. Standardized method for in vitro antifungal susceptibility testing of *Candida albicans* biofilms. Antimicrob. Agents Chemother. 45:2475–2479.
16. **Kaneko Y, Ohno H, Kohno S, Miyazaki Y.** 2010. Micafungin alters the expression of genes related to cell wall integrity in *Candida albicans* biofilms. Jpn. J. Infect. Dis. 63:355–357.
17. **Mukherjee PK, Zhou G, Munyon R, Ghannoum MA.** 2005. *Candida* biofilm: a well-designed protected environment. Med. Mycol. 43:191–208.
18. **Valentín A, Canton E, Peman J, Martinez JP.** 2012. Voriconazole inhibits biofilm formation in different species of the genus *Candida*. J. Antimicrob. Chemother. 67:2418–2423.
19. **Ramage G, VandeWalle K, Bachmann SP, Wickes BL, Lopez-Ribot JL.** 2002. In vitro pharmacodynamic properties of three antifungal agents against preformed *Candida albicans* biofilms determined by time-kill studies. Antimicrob. Agents Chemother. 46:3634–3636.

Downloaded from http://aac.asm.org/ on February 3, 2014 by National Institute of Infectious Diseases, Murayama Bunshitsu